International Journal of
Molecular Sciences

MDPI

Article

Self-Organization of Fullerene Derivatives in Solutions and Biological Cells Studied by Pulsed Field Gradient NMR

Irina A. Avilova [1], Alexander V. Chernyak [1,2], Yuliya V. Soldatova [1], Alexander V. Mumyatov [1], Olga A. Kraevaya [1], Ekaterina A. Khakina [3], Pavel A. Troshin [1] and Vitaliy I. Volkov [1,2,*]

[1] Federal Research Center for Problems of Chemical Physics and Medicinal Chemistry RAS, 142432 Chernogolovka, Russia
[2] Scientific Center in Chernogolovka RAS, 142432 Chernogolovka, Russia
[3] A.N. Nesmeyanov Institute of Organoelement Compounds RAS, 119334 Moscow, Russia
* Correspondence: vitwolf@mail.ru

Abstract: Fullerene derivatives are of great interest in various fields of science and technology. Fullerene derivatives are known to have pronounced anticancer and antiviral activity. They have antibacterial properties. Their properties are largely determined by association processes. Understanding the nature and properties of associates in solvents of various types will make it possible to make significant progress in understanding the mechanisms of aggregation of molecules of fullerene derivatives in solutions. Thus, this work, aimed at studying the size and stability of associates, is relevant and promising for further research. The NMR method in a pulsed field gradient was used, which makes it possible to directly study the translational mobility of molecules. The sizes of individual molecules and associates were calculated based on the Stokes–Einstein model. The lifetime of associates was also estimated. The interaction of water-soluble C_{60} fullerene derivatives with erythrocytes was also evaluated. The values of self-diffusion coefficients and the lifetime of molecules of their compounds in cell membranes are obtained. It is concluded that the molecules of fullerene derivatives are fixed on the cell surface, and their forward movement is controlled by lateral diffusion.

Keywords: fullerene derivatives; associates; solution; red blood cells; pulsed field gradient NMR; self-diffusion; lifetime; lateral diffusion

Citation: Avilova, I.A.; Chernyak, A.V.; Soldatova, Y.V.; Mumyatov, A.V.; Kraevaya, O.A.; Khakina, E.A.; Troshin, P.A.; Volkov, V.I. Self-Organization of Fullerene Derivatives in Solutions and Biological Cells Studied by Pulsed Field Gradient NMR. *Int. J. Mol. Sci.* **2022**, *23*, 13344. https://doi.org/10.3390/ijms232113344

Academic Editor: Victor V. Nikonenko

Received: 8 October 2022
Accepted: 28 October 2022
Published: 1 November 2022

1. Introduction

Fullerene is a three-dimensional allotropic modification of carbon (C_n, where n = 20 . . . 540). A fullerene molecule is a convex closed polyhedron consisting of an even number of atoms forming pentagons and hexagons. Currently, a large number of types of fullerenes are known, but the most common and studied is the C_{60} molecule. At the vertices of a truncated icosahedron are 60 carbon atoms, and the faces are 20 hexagons and 12 pentagons. Fullerene derivatives are widely used in various fields of science and technology [1,2].

Water-soluble fullerene derivatives (WSFD) show considerable promise in the field of biomedical applications. These are substances with unique properties. They can be used as a targeted component of drug delivery systems. It is known from the literature data that some of the fullerene derivatives exhibited pronounced anticancer activity [3–6], antiviral (including anti-HIV) [7–11], and antibacterial [4,12,13] activity. It was also shown that fullerenes and fullerene-dye hybrid structures have a pronounced antitumor photodynamic effect [14–16].

The biological activity of water-soluble fullerene derivatives is explained by the peculiarity of their structure. Water-soluble fullerene derivatives are amphiphilic compounds consisting of a hydrophobic carbon framework surrounded by hydrophilic addends [17–19]. As a result, these compounds are lipophilic. On the one hand, WSFDs interact with the lipid matrix of the cell membrane; on the other hand, WSFDs interact specifically with protein active sites.

There are many publications devoted to the behavior of WSFD in proteins, model and native biological membranes [20–24]. However, at the same time, only a few works are devoted to studying the interaction of water-soluble fullerene derivatives with red blood cell (RBC) membranes [25,26]. Although RBCs as a biological system are of interest since the structure of their membrane is similar to the membranes of other cells. In [25,26], fullerenols $C_{60}(OH)_{24}$ and $C_{60}(OH)_{36}$ containing polar hydroxyl groups were studied. The authors showed that fullerenols are predominantly associated with surface proteins of the plasma membrane; however, they can also be incorporated into the membrane. It has also been demonstrated that fullerenol affects membrane ATPases and can modulate ion transport across membranes.

The amphiphilic nature of the molecules of water-soluble fullerene derivatives causes their aggregation in aqueous solutions. As a result of self-organization processes, nanosized hollow spherical vesicles are formed [27–29]. It is reasonable to assume that the biological properties of these molecules will be influenced by the processes of self-aggregation and the size of the resulting clusters. Therefore, the study of self-organization in solutions of fullerene derivatives is of fundamental importance.

The processes of self-organization of fullerene derivatives in water and organic solutions are studied using various experimental methods: dynamic light scattering [7,30–32], atomic force microscopy [7,30,33,34], transmission electron microscopy [7,32,33,35,36]. However, these methods are rather indirect.

The most direct way to estimate the size of aggregates in solutions from diffusion coefficients is using the Stokes–Einstein model. Diffusion NMR spectroscopy is informative for measuring molecular diffusion parameters [37,38]. For example, in [39–42], the ^{1}H DOSY NMR method was used to study supramolecular systems based on fullerenes. This method made it possible to obtain information about the processes of formation of supramolecular systems by analyzing the self-diffusion coefficients of the initial compounds and finished complexes. It was shown that the mobility of supramolecular systems is lower than the mobility of the initial molecules. In paper [43], the ^{1}H DOSY NMR method was used to establish the formation of fullerene polyesters, which was also confirmed by a decrease in the diffusion coefficient.

A special place in the field of diffusion NMR spectroscopy is occupied by the pulsed field gradient NMR technique (PFG NMR). In the PFG NMR experiment, individual diffusion components could be selected from the NMR spectra using Fourier transform, and the partial diffusion coefficients can be estimated, which makes it possible to apply this method to study the association of fullerene derivatives in organic and aqueous media.

Another remarkable feature of PFG NMR is the possibility of its application to study the translational mobility of molecules in biological systems (cells, models) [22,23,44–53]. It does not have a destructive effect on cells and, at the same time, allows obtaining of qualitative and quantitative information related to the self-diffusion processes of molecules in biosystems.

Thus, the following conclusions can be drawn. First, water-soluble fullerene derivatives are promising compounds for biomedical research and pharmaceutical applications. Second, the investigation of these substances' state in aqueous solutions, as well as their interaction with biological systems (for example, RBCs), is very important. Third, the pulsed field gradient NMR technique makes it possible to noninvasively study the translational mobility of fullerene derivatives molecules in solutions and biological cells.

Herein we have presented the experimental results of fullerene derivative association in solutions and erythrocytes obtained with the pulsed field gradient technique.

2. Results and Discussion

2.1. Fullerene Derivatives in Solutions

The Stokes–Einstein model is usually used to describe the aggregation of molecules in solutions. The hydrodynamic radius r_H of a spherical particle is calculated using the self-diffusion coefficient D according to Equation (1) [54–58]:

$$D = \frac{k \cdot T}{n \cdot \pi \cdot \eta \cdot r_H}, \quad (1)$$

where k is the Boltzmann constant, T is the absolute temperature, and η is the solvent viscosity.

In the case of slip molecules, the value of n is equal to four. For the stick-shaped molecules, n is equal to 6.

The applicability of the Stokes–Einstein model for calculating the size of particles formed by molecules of fullerene derivatives was tested using the fluorinated fullerene $C_{60}F_{36}$. The structure of this compound is well known; the van der Waals diameter is 1.23 nm [58]. From the experimental data of PFG NMR of ^{19}F nuclei, the value of the self-diffusion coefficient of $C_{60}F_{36}$ molecules was obtained, which was 6.5 10^{-10} m^2/s [59]. The hydrodynamic diameter $2r_H$, calculated from Equation (1), is equal to the van der Waals diameter at n = 6 within the measurement error. Thus, it seems appropriate to apply Equation (2) for hydrodynamic radii of particles formed by molecules of fullerene derivatives estimation:

$$r_H = \frac{k \cdot T}{6 \cdot \pi \cdot \eta \cdot D} \quad (2)$$

2.1.1. Nonpolar Fullerene Derivatives

The molecular structures of fullerene derivatives that do not contain polar groups (**I–V**) are shown in Figure 1.

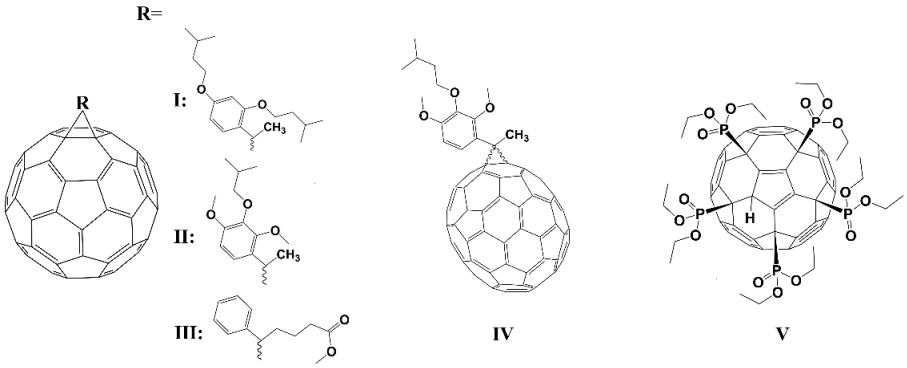

Figure 1. The molecular structure of compounds **I–V**.

For compounds **I–V**, spin echo attenuation of ^1H nuclei was measured in the solvents indicated in Section 3.1. The dependences of the spin echo attenuation amplitude $A(2\tau, \tau_1, g)$ vs. the square of the pulsed field gradient amplitude g^2 (diffusion decays) were analyzed. The diffusion decays were exponential shapes and fitted well using Equation (3):

$$A(2\tau, \tau_1, g) = A(2\tau, \tau_1, 0) exp\left(-\gamma^2 g^2 \delta^2 t_d D_s\right), \quad (3)$$

which is an instance of Equation (9) presented in Section 3.3 at m = 1.

The exponential character of diffusion decays of compounds **I–V** indicates that the mobility of the molecules of fullerene derivatives is characterized by a single self-diffusion coefficient D_s. Since the NMR spectra of the studied compounds are well resolved, the diffusion decays of different spectral lines belonging to different functional groups were analyzed. The resulting decays turned out to be almost identical.

Table 1 presents the self-diffusion coefficients obtained for the molecules of compounds **I–V** in various solvents. The sizes of particles $d_H = 2 \cdot r_H$ are calculated using the Stokes–Einstein Equation (2).

Table 1. The self-diffusion coefficients D_s and the diameters d_H calculated from Equation (2) for the fullerene derivatives **I–V**.

Compound	Solvent	D_s, m^2/s	d_H, nm
I	$CDCl_3$	$5.9 \cdot 10^{-10}$	1.3 ± 0.1
	CS_2	$1.0 \cdot 10^{-9}$	1.2 ± 0.1
II	$CDCl_3$	$6.3 \cdot 10^{-10}$	1.3 ± 0.1
	CS_2	$1.1 \cdot 10^{-9}$	1.2 ± 0.1
	$C_6D_5CD_3$	$6.6 \cdot 10^{-10}$	1.2 ± 0.1
III	$CDCl_3$	$6.9 \cdot 10^{-10}$	1.2 ± 0.1
IV	$C_6D_5CD_3$	$6.1 \cdot 10^{-10}$	1.2 ± 0.1
V	$CDCl_3$	$5.8 \cdot 10^{-10}$	1.4 ± 0.1

The hydrodynamic diameters of the molecules of compounds **I–V** are in the range of 1.2–1.4 nm. It should be noted that the type of solvent does not affect the particle sizes, which are close to the van der Waals diameter of the fullerene. Thus, fullerene derivatives containing non-polar groups are not prone to the formation of aggregates but are in solutions as isolated molecules.

2.1.2. Polar Fullerene Derivatives

Another picture was observed for fullerene derivatives containing polar groups. The molecular structures of fullerene derivatives containing polar groups are shown in Figure 2.

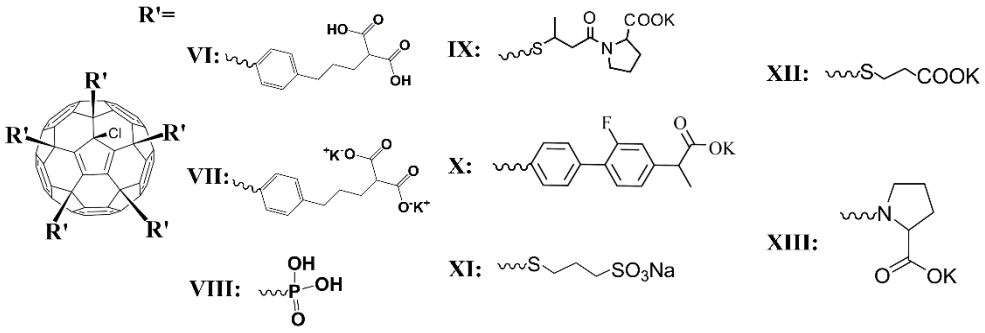

Figure 2. The molecular structure of compounds **VI–XIII**.

The exponential diffusion decays were observed for solutions of **VI** in deuterated DMSO-d_6, acetone-d6, and DMSO-D_2O mixtures. The fullerene self-diffusion coefficients and hydrodynamic diameters calculated from Equations (2) and (3), respectively, are shown in Table 2.

The calculated particle size formed by the molecules of compound **VI** in solutions of deuterated DMSO and acetone was 2.3–2.4 nm. The obtained value exceeds the size of the C60 fullerene molecule twice as much. Presumably, it can be explained by the presence of five bulk addends on the C_{60} fullerene framework, which increases the molecular hydrodynamic diameter. Another option is the formation of self-assembling dimers by compound **VI** due to the occurrence of hydrogen bonds between the -COOH groups of two complementary molecules, as is well known for organic acids.

Table 2. The self-diffusion coefficients D_s and the diameters d_H from Equation (2) for fullerene derivative **VI**, the solution concentration C = 8 mg/mL.

Solvent	D_s, m^2/s	d_H, nm
acetone-d6	$5.7 \cdot 10^{-10}$	2.4 ± 0.2
DMSO	$8.5 \cdot 10^{-11}$	2.3 ± 0.2
The molar ratio DMSO:D_2O = 3:1	$2.1 \cdot 10^{-11}$	5.4 ± 0.5
The molar ratio DMSO:D_2O = 1:1	$2.3 \cdot 10^{-11}$	6.3 ± 0.6
The molar ratio DMSO:D_2O = 1:3	$2.3 \cdot 10^{-11}$	9.6 ± 0.9

At the same time, in a mixture of DMSO-D_2O solvents, for the molecules of compound **VI**, a noticeable aggregation was observed, which can be seen in Table 2. Probably, stable aggregates of various sizes, including D_2O molecules, are formed in the system. In addition, the observed exponential diffusion decay characterizes an average aggregate self-diffusion coefficient.

Associates formed by the molecules of compound **VI** possess low stability, which was confirmed using the dependence of the hydrodynamic diameter d_H on temperature. Figure 3 shows that with the increasing temperature of the solution from 25 to 45 °C, a decrease in particle size was observed.

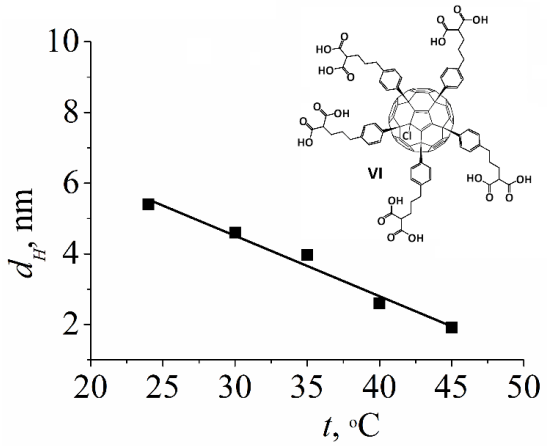

Figure 3. Temperature dependence of the hydrodynamic diameter d_H characterizing the association of the fullerene derivative **VI** in DMSO/D_2O (3:1 m/m) solution. The concentration of **VI** was 8 mg/mL.

2.1.3. Water-Soluble Fullerene Derivatives

The results obtained for compounds **VII**–**XIII** in aqueous solutions should be considered separately.

Compound **VII**

Water-soluble fullerene derivatives (e.g., compound **VII** in Figure 2) demonstrate the strongest tendency to self-organization in solutions. The self-diffusion of the potassium salt **VII** in D_2O was investigated. The diffusion decays were approximated by the sum of two exponential components according to Equation (4) [59] (m is equal to two in Equation (9)) as it is shown in Figure 4:

$$A(g) = p_1 \exp\left(-\gamma^2 g^2 \delta^2 t_d D_{s1}\right) + p_2 \exp\left(-\gamma^2 g^2 \delta^2 t_d D_{s2}\right), \quad (4)$$

where p_1, D_{s1} and p_2, D_{s2}—are the relative parts (phase populations) and partial self-diffusion coefficients of the first and the second component, respectively.

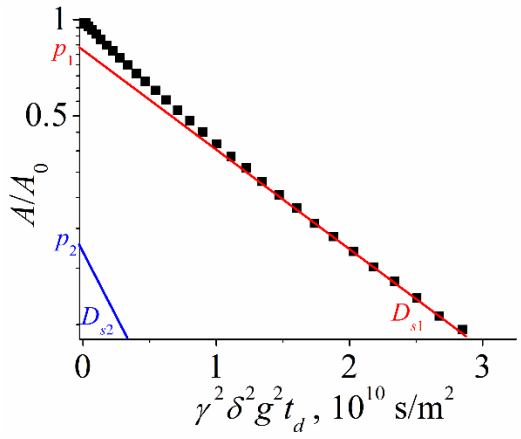

Figure 4. Diffusion decay of the fullerene derivative **VII** in D_2O solution at t_d = 20 ms, C = 6 mg/mL.

The hydrodynamic diameters d_H based on each self-diffusion coefficient were calculated from Equation (2) and are given in Table 3.

Table 3. The self-diffusion coefficients D_{s1}, D_{s2}, populations p_1, p_2, and the hydrodynamic diameters d_{H1}, d_{H2} of the aggregates formed by the compound **VII** in deuterated water solutions.

C, mg/mL	D_s, m²/s		p		d_H, nm	
	D_{s1}	D_{s2}	p_1	p_2	d_{H1}	d_{H2}
6	$7.1 \cdot 10^{-11}$	$2.1 \cdot 10^{-10}$	0.60	0.40	5.5 ± 0.5	1.8 ± 0.2
12	$6.6 \cdot 10^{-11}$	$1.7 \cdot 10^{-10}$	0.70	0.30	5.9 ± 0.6	2.3 ± 0.2
14	$7.1 \cdot 10^{-11}$	$1.7 \cdot 10^{-10}$	0.80	0.20	5.5 ± 0.5	2.3 ± 0.2
24	$6.9 \cdot 10^{-11}$	$2.0 \cdot 10^{-10}$	0.87	0.13	5.7 ± 0.6	1.9 ± 0.2

From the data in Table 3, we can conclude that there are two different types of clusters formed by the fullerene derivative in the solution. Based on the obtained values of hydrodynamic diameters, it can be assumed that isolated molecules (d_H = 2 nm) and stable aggregates (d_H about 5.5 nm) are observed. The values of the self-diffusion coefficients did not depend on the solution concentration; they were constant in the concentration range from 6 to 24 mg/mL. The increasing of aggregate populations with concentration rising was observed.

Compound **VIII**

The results obtained for the fullerene derivative **VIII** show a completely different behavior of molecules in the solution. It is assumed that for the molecules of this compound, the aggregate lifetime is shorter than the diffusion time. This ensures fast exchange between isolated molecules and aggregates of compound **VIII**. Therefore, the obtained diffusion decays are exponential. Their analysis revealed average self-diffusion coefficients characterizing the translational mobility of various types of compound **VIII** aggregates.

Figure 5 shows the dependence of the self-diffusion coefficient of molecules of compound **VIII** on the concentration of an aqueous solution. At low solution concentrations (less than 3 mg/mL), the d_H value was (1.3 ± 0.15) nm, which corresponds to the size of an isolated molecule. With an increase in concentration, a decrease in the self-diffusion coefficient was observed, which indicates the formation of aggregates by the molecules of the fullerene derivative **VIII**. At a solution concentration of 40 mg/mL, the maximum value of the hydrodynamic diameter d_H = (4.5 ± 0.5) nm was obtained, which does not change with a further increase in concentration.

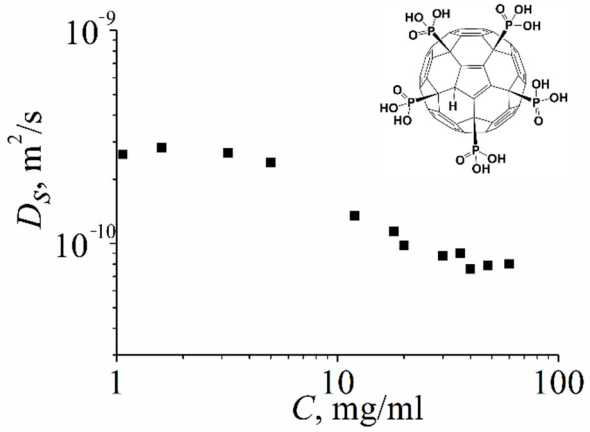

Figure 5. The concentration dependence of self-diffusion coefficients of compound **VIII** in D_2O measured on ^{31}P nuclei.

Compound **IX**

For compound **IX**, aqueous solutions of the concentrations indicated in paragraph 4.1 were prepared, and NMR experiments were performed. The diffusion decays of fullerenes (Figure 6) were approximated using bi-exponential curves according to Equation (4).

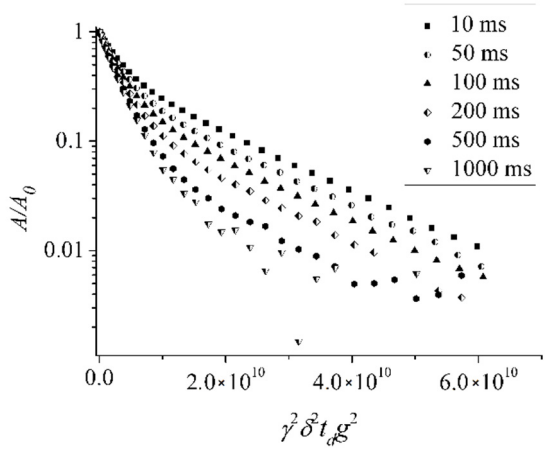

Figure 6. Diffusion decays of the fullerene derivative **IX** at different diffusion times t_d. The values of t_d are indicated in insertion. C = 64.4 mg/ml. Reprinted with permission from Ref. [37]. Copyright © 2016 Published by Elsevier B.V.

From the analysis of diffusion decays, the self-diffusion coefficients of the molecules of compound **IX** were obtained, the values of which were $Ds_1 = (6.5 \pm 0.3)\ 10^{-11}$ m^2/s and $Ds_2 = (4.0 \pm 0.5)\ 10^{-10}$ m^2/s.

By analogy with the previous compounds, it is assumed that Ds_1 and Ds_2 characterize particles of the fullerene derivative of different sizes. From Equation (2), the particle sizes were calculated, the values of which were $d_{H1} = (5.2 \pm 0.4)$ nm and $d_{H2} = (1.0 \pm 0.06)$ nm. The obtained values indicate that the molecules of compound **IX** in an aqueous solution are represented by isolated and aggregated molecules.

The experimental data obtained for compound **IX** give the possibility to estimate the lifetime of aggregates formed by molecules in an aqueous solution. The lifetime of fullerene aggregates was estimated from the temperature dependence of the low self-diffusion coefficient population on diffusion time t_d $p_2(t_d)$ according to the procedure proposed in [37].

Figure 7 shows an example of dependence $p_2(t_d)$. The characteristic times of the curve tail were about 1 s, which was in good agreement with the values of the spin lattice relaxation times (T_1 = 0.9 s) for this compound, measured independently. Figure 7 also

shows the result of the spin lattice relaxation component subtracting, which is a straight line. Their slopes were used to calculate the lifetime τ according to Equation (5):

$$p_2 = p_f \exp\left(-\frac{t_d}{\tau}\right) + p_s \exp\left(-\frac{t_d}{T_1}\right), \quad (5)$$

where τ is the lifetime, T_1 is fullerene spin lattice relaxation time, $p_f + p_s = p_2(0)$.

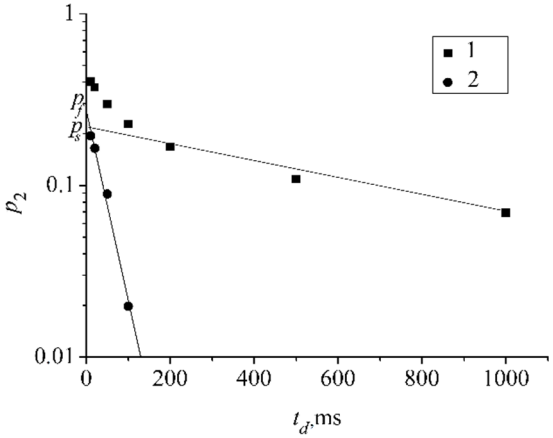

Figure 7. 1—the dependence of part $p_2(t_d)$ on diffusion time t_d; 2—the dependence $p_2(t_d)$ after subtraction of spin–lattice relaxation component. Reprinted with permission from Ref. [37]. Copyright © 2016 Published by Elsevier B.V.

The lifetime values τ are 140 ms, 180 ms, and 200 ms for compound **IX** solution concentrations of 64.4 mg/mL, 21.3 mg/mL, and 5.3 mg/mL, respectively.

Compound **X**

For compound **X**, aqueous solutions of the concentrations indicated in Section 3.1 were prepared. NMR studies were performed for ^{1}H and ^{19}F nuclei. The diffusion decays of ^{1}H (Figure 8a) and ^{19}F (Figure 8b) nuclei at different diffusion times t_d are shown.

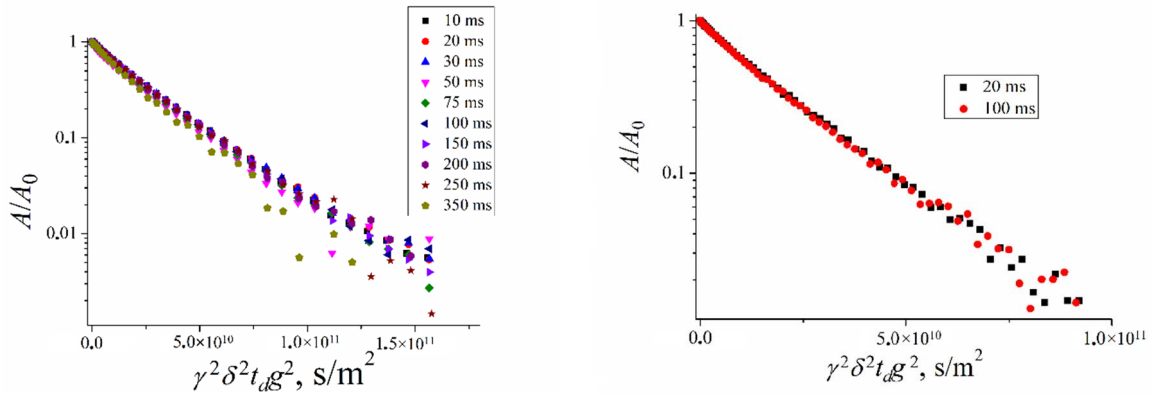

Figure 8. 10 Diffusion decays of ^{1}H and ^{19}F nuclei of compound **X** at different diffusion times t_d: (**a**)—^{1}H nuclei; (**b**)–^{19}F nuclei. The values of t_d show in insertions. The aqueous solution concentration is 50 mg/mL.

These diffusion decays are bi-exponential shapes. As shown in Figure 8, self-diffusion coefficients D_{s1} and D_{s2} are t_d independent. It may be proposed that two types of molecule associations are observed. The exchange rate between these two associates was slow compared to diffusion time. Self-diffusion coefficients decrease with solution concentration increasing. Hydrodynamic diameters calculated from Stokes–Einstein by Equation (2) are

given in Table 4. The lesser diameter is close to individual molecule diameters, but the largest diameter characterizes associate size.

Table 4. Diameters of particles of compound **X** calculated on the basis of Equation (2) from self-diffusion coefficients measured for ^{1}H and ^{19}F nuclei.

C, mg/mL	^{1}H		^{19}F	
	d_{H1}, nm	d_{H2}, nm	d_{H1}, nm	d_{H2}, nm
6	7.6 ± 0.4	0.8 ± 0.1	7.6 ± 0.4	1.0 ± 0.1
8	7.6 ± 0.4	1.0 ± 0.1	7.8 ± 0.4	1.0 ± 0.1
12	7.4 ± 0.4	1.1 ± 0.1	8.2 ± 0.4	1.1 ± 0.1
16	7.6 ± 0.4	1.1 ± 0.1	8.0 ± 0.4	1.1 ± 0.1
24	8.0 ± 0.4	1.3 ± 0.1	8.4 ± 0.4	1.6 ± 0.1
30	7.9 ± 0.4	1.5 ± 0.1	8.8 ± 0.4	1.9 ± 0.1
50	9.8 ± 0.4	2.4 ± 0.1	10.6 ± 0.4	2.4 ± 0.1

The particle sizes calculated from ^{1}H and ^{19}F self-diffusion data are agreed well. The associate size, as well as the relative part of associated molecules, increases with the solution concentration increasing. The diameter increases from 7.6 nm to 9.8 nm and from 7.6 nm to 10.6 nm; the associate part increases from 0.67 to 0.8 and from 0.69 to 0.83 for ^{1}H and ^{19}F data, correspondingly, with concentration increasing from 6 to 50 mg/mL.

Compound **XI**

For compound **XI**, aqueous solutions of the concentrations indicated in Section 3.1 were prepared. NMR studies were performed on ^{1}H nuclei. These derivative diffusion decays are bi exponential which was evidence of two sizes of particles: individual molecules d_{H2} = (0.9 ± 0.1) nm and associated molecules d_{H1} = (5.6 ± 0.3) nm.

As shown in Figure 9, the low diffusion associated molecule component population p_1 decreases with diffusion time t_d increasing. In Figure 9, $p_1(t_d)$ dependence is shown.

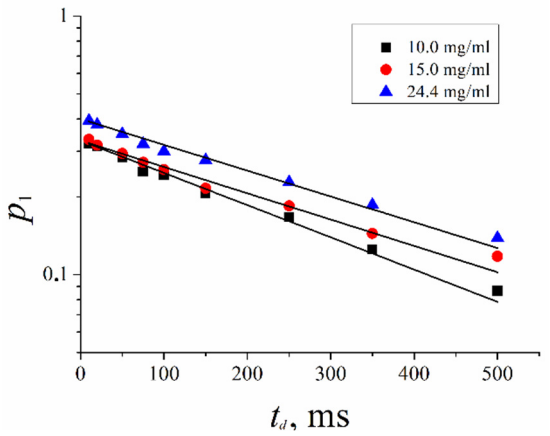

Figure 9. Dependences of associate molecules populations of compound **XI** on diffusion times. The values of concentrations are indicated in insertion.

This dependence is exponential, as described by Equation (6). The lifetime of associates formed by molecules of compound **XI** in aqueous solutions was calculated.

$$p(t_d) = p(0)\exp\left(-\frac{t_d}{\tau}\right) \quad (6)$$

The lifetime of associates τ are (350 ± 10), (430 ± 20) and (440 ± 20) ms at solution concentration C = 10, 15 and 24.4 mg/mL, accordingly. The lifetime of associates increased insignificantly with solution concentration increasing.

Compound **XII**

The diffusion decay of compound **XII** is bi-exponential, which is due to isolated (self-diffusion coefficient D_{s2} = (4.3 ± 0.8)·10^{-10} m^2/s) and associated molecules (self-diffusion coefficient D_{s1} = (7.5 ± 1.5)·10^{-11} m^2/s). The dependence of diffusion decay shape on diffusion time t_d and concentration was negligible, indicating a slow exchange between isolated and associated molecules compared to the maximum value of t_d (250 ms). The isolated molecule size d_{H2} = 1.0 ± 0.2 nm, and the associate size was d_{H1} = 5.0 ± 1.0 nm. The relative part of associates increases with concentration growth from 0.56 to 0.73.

Compound **XIII**

The ^{1}H diffusion decay for molecules of compound **XIII** is also bi-exponential, and decay shape depends on diffusion time and solution concentration C insignificantly. Self-diffusion coefficients Ds_1 and Ds_2 are (1.3 ± 0.1)·10^{-10} m^2/s and (5.8 ± 0.2)·10^{-10} m^2/s, accordingly. Hydrodynamical diameters are d_{H2} = (0.7 ± 0.1) nm—isolated molecules and d_{H1} = (2.8 ± 0.2) nm—associates. The associated molecules' relative part increases from 0.59 to 0.70, with concentration increasing from 3 to 40 mg/mL.

2.2. Water-Soluble Fullerene Derivatives in Red Blood Cells

Water-soluble fullerene derivatives (WSFDs) are biologically active species. Therefore, one of the fundamental problems is to reveal the mechanism of fullerene derivative interaction with Red Blood Cells (RBCs).

We have previously performed a detailed study of the translational mobility of compound **XI** in various biological systems: liposomes, shadows, and erythrocytes [53]. In this work, analysis of the high-resolution NMR spectra of the following systems was conducted: an aqueous solution of compound **XI**; RBCs suspension; suspensions of RBCs, RBCs shadows, and liposomes with the addition of compound **XI**. Using the analysis of ^{1}H spectra at different amplitudes of the magnetic field gradient, we showed that the signals from the protons of compound **XI** could be uniquely identified in the spectra of suspensions. These signals do not overlap with the proton signals of the membrane components. It was also shown that, at a high amplitude of the magnetic field gradient, in the spectra of ^{1}H suspension of RBCs with added compound **XI**, a signal of WSFD molecules was well observed. At the same time, proton signals of compound **XI** molecules are absent in an aqueous solution under the same experimental conditions. A similar picture was obtained for compounds **XII** and **XIII**. Figure 10 shows examples of the ^{1}H spectra of the systems under study (erythrocyte suspensions with added compounds **XI**–**XIII**). ^{1}H chemical shifts of compounds are slightly changing in suspensions of RBCs compared to solutions due to fullerene derivative interaction with RBCs.

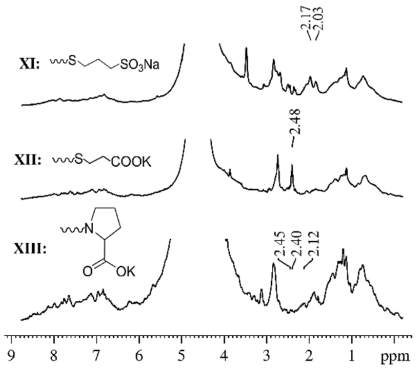

Figure 10. The ^{1}H spectra of the RBCs suspensions with added compounds **XI**–**XIII**.

The isolated ^{1}H signals of compound molecules give the possibility to register the diffusion decays of WSFD molecules in a suspension of RBCs correctly. The obtained experimental data made it possible to extract information about the translational mobility of WSFD molecules in cell suspensions. The obtained diffusion decays were complex and were decomposed into three exponent components according to Equation (9) at $m = 3$. At the same time, in aqueous solutions of compounds **XI–XIII**, two exponential diffusion decays are observed. The values of the self-diffusion coefficients of the molecules of compounds **XI–XIII** are presented in Table 5 [44].

Table 5. Self-diffusion coefficients of WSFD molecules in aqueous solutions and RBCs suspension. $D_{s1}{}^{w}$ and $D_{s2}{}^{w}$—aqueous solution; $D_{s1}{}^{s}$, $D_{s2}{}^{s}$, $D_{s3}{}^{s}$—RBCs suspension. Reprinted with permission from Ref. [44].

Compound	Aqueous Solution		RBCs Suspension		
	$D_{s1}{}^{w}\cdot10^{11}$, m^2/s	$D_{s2}{}^{w}\cdot10^{10}$, m^2/s	$D_{s1}{}^{s}\cdot10^{12}$, m^2/s	$D_{s2}{}^{s}\cdot10^{11}$, m^2/s	$D_{s3}{}^{s}\cdot10^{10}$, m^2/s
XI	7.4 ± 0.7	4.1 ± 0.4	5.5 ± 0.8	3.9 ± 0.6	5.5 ± 0.8
XII	7.5 ± 1.5	4.3 ± 0.8	5.0 ± 1.0	4.4 ± 0.9	7.1 ± 1.4
XII	4.9 ± 0.5	1.2 ± 0.1	6.0 ± 1.0	3.8 ± 0.6	8.0 ± 1.0

As shown in Table 5, the translational mobility of molecules of compounds **XI–XIII** in a suspension of RBCs is characterized by three diffusion coefficients, the values of which differ by an order of magnitude. However, only two self-diffusion coefficients have been identified in the aqueous solutions of these compounds. Extraction of the third coefficient of self-diffusion, the value of which differs significantly from the other two coefficients, suggests that the movement of the molecules of compounds **XI–XIII** in the cell suspension was hindered.

It is known from the literature data that the lateral diffusion coefficient D_L, which characterizes the mobility of lipid molecules in the cell membrane, has a value of about (5–7)$\cdot10^{-12}$ m^2/s [44,52,53]. The observed "low" coefficient of self-diffusion of the molecules of compounds **XI–XIII** was close to a lateral diffusion coefficient. Thus, the complex nature of the obtained experimental data can be explained by the fact that in the erythrocyte suspension, the molecules of compounds **XI–XIII** are in the aqueous phase of the system or are bound to the erythrocyte cell membrane. The penetration of molecules of compounds **XI–XIII** into the membrane was observed as a result of the appearance of a slow diffusion component. At the same time, in the aqueous phase, the molecules of compounds **XI–XIII** are in an isolated and associated form.

The analysis of the dependence of relative parts slow moving fullerene derivative molecules p_1 on diffusion time t_d makes it possible to estimate the lifetimes τ of fullerene derivative molecules in the erythrocyte membrane from Equation (6). Lifetimes τ for compounds **XI–XIII** are given in Table 6.

Table 6. The self-diffusion coefficients $D_{s1}{}^{s}$, population p_1 at $t_d \to 0$, $p_1(0)$, and lifetimes τ of WSFD molecules in RBCs. Reprinted with permission from Ref. [44].

Compound	$D_{s1}{}^{s}\cdot10^{12}$, m^2/s	$p_1(0)$	τ, ms
XI	5.5 ± 0.8	0.33	440 ± 70
XII	5.0 ± 1.0	0.13	470 ± 70
XIII	6.0 ± 1.0	0.06	1200 ± 300

The dependences of the relative parts p_1 of molecules of compound **XI** on the diffusion time t_d at different concentrations are shown in Figure 11. From the analysis of these dependences, the lifetime calculation was carried out according to Equation (6). The obtained values of the lifetimes are presented in Table 7.

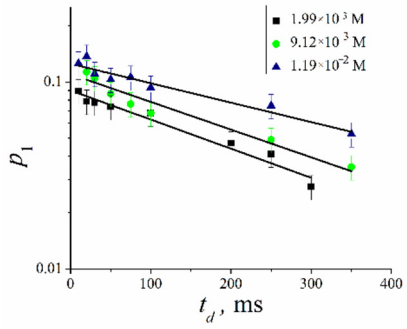

Figure 11. The dependences of the relative parts p_1 of molecules of compound **XI** on the diffusion time t_d at various concentrations. The concentrations indicate in the insertion.

Table 7. The values of the lifetime of the molecules of compound **XI** in the RBC membrane at various concentrations.

C, M	τ_1, ms
$1.99 \cdot 10^{-3}$	280 ± 15
$9.12 \cdot 10^{-3}$	300 ± 20
$1.19 \cdot 10^{-2}$	440 ± 70

As seen from Table 7, the lifetime τ_1 of compound **XI** molecules in the cell membrane increases with the increase of its concentration in the RBCs suspension.

3. Materials and Methods

3.1. Fullerene Derivatives

Methanofullerenes **I**, **II,** and **IV** were reported recently [60,61]. Compound **III** represents a well-known n-type material for organic solar cells abbreviated as PCBM [62]. Fullerene derivatives **V** and **VIII** were synthesized recently in the reaction of chlorofullerene $C_{60}Cl_6$ and triethyl phosphite [17]. Fullerene derivatives **VI** and **VII** were reported as products of the Friedel–Crafts arylation of $C_{60}Cl_6$ [63]. Compounds **IX and XI** were synthesized as described in [64]. Fullerene derivatives **X**, **XII**, and **XIII** were obtained and characterized as reported in our previous papers [19], [65], [66], respectively.

The molecular mobility of compounds **I**–**V** was studied in various solvents: $CDCl_3$ (**I**, **II**, **III**, **V**), CS_2 (**I**, **II**), and $C_6D_5CD_3$ (**II**, **IV**). For investigation of the molecular mobility of compound **VI** in solution, deuterated DMSO-d6, acetone-d6, and mixtures of DMSO-D_2O were used. Compounds **VII**–**XIII** are highly soluble in water due to the presence of five hydrophilic groups. Therefore, solutions of various concentrations in deuterium water were prepared for them. The concentrations were from 6 to 24 mg/mL for **VII**; from 2 to 50 mg/mL for **VIII**; from 5 to 64 mg/mL for **IX**; from 6 to 50 mg/mL for **X**; from 10 to 24 mg/mL for **XI**; from 10 to 47 mg/mL for **XII**; from 3 to 40 mg/mL for **XIII**.

3.2. Red Blood Cells

Blood samples were taken from anesthetized mice by decapitation. The 0.11 molar sodium citrate aqueous solutions were used as an anticoagulant. The citrate solution to blood ratio was one to five by volume. The collected blood samples were centrifuged for 15 min at 1000 rpm, and the plasma was removed with decantation. The erythrocyte sediment was resuspended in NaCl solution (salt concentration was 0.85 g per 100 mL) containing 5 mM of Na-phosphate buffer with pH = 7.4. The centrifugation and decantation procedures were repeated triply; the duration of the second and third centrifugations was 7 min. The fresh buffered NaCl solution was used for each resuspending step. The obtained erythrocyte sediment was stored at 4 °C for no more than 36 h. The fullerene derivatives were added to the RBCs suspension. The final concentration of WSFD in suspension

was $1.19 \cdot 10^{-2}$, $9.12 \cdot 10^{-3}$, and $1.99 \cdot 10^{-3}$ M for compound **XI**; $1.2 \cdot 10^{-2}$ M for compound **XII** and **XIII**.

3.3. PFG NMR Technique

The self-diffusion coefficients were measured with the pulsed field gradient technique for ^{1}H, ^{19}F, and ^{31}P nuclei at the frequencies of 400.13, 376.498, and 161.976 MHz, correspondingly. The measurements were conducted on Bruker Avance-III—400 NMR spectrometer equipped with the diff-60 gradient unit. The pulsed field gradient stimulated echo sequence shown in Figure 12 was applied in the experiments. Three 90° pulses produce a stimulated spin-echo at the time of $2\tau + \tau_1$ (where τ and τ_1 are the time intervals between the first and the second or the second and the third 90° pulses, respectively). The magnetic field gradient pulses of amplitude g and duration δ were applied after the first and the third 90° pulses. The gradient strength was varied linearly in 64 steps within the range from 0.1 to 27 T/m. The integrated intensities of the spectrum lines were used to obtain the dependence of the echo signal attenuation with respect to g^2 (diffusion decay) [44,49–52,67].

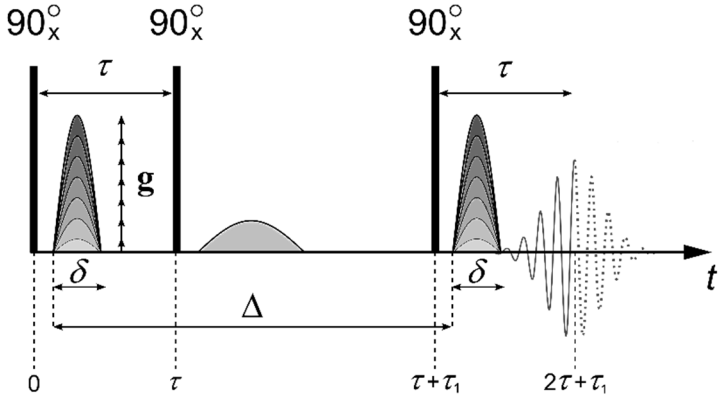

Figure 12. Stimulated echo pulse sequence with the magnetic field gradient pulses. Here, τ is the time interval between the first and the second RF pulses, and τ_1 is the time interval between the second and the third ones. D is the interval between the gradient pulses, δ is the duration of the equivalent rectangular magnetic field gradient pulses, g is the amplitude of the magnetic field gradient pulse, and g_0 is the amplitude of the constant magnetic field gradient. Reprinted with permission from Ref. [44].

For the molecules undergoing unhindered isotropic Brownian motion, the evolution of the spin echo signal is described by the following Equation (3):

$$A(2\tau, \tau_1, g) = A(2\tau, \tau_1, 0) exp\left(-\gamma^2 g^2 \delta^2 t_d D_s\right), \quad (3)$$

where γ is gyromagnetic ratio, $t_d = \Delta - \delta/3$ is the diffusion time, and D_s is the self-diffusion coefficient, τ, τ_1 and g are shown in Figure 12; $A(2\tau, \tau_1, 0)$ is expressed by the equation:

$$(2\tau, \tau_1, 0) = \frac{A(0)}{2exp\left(-\frac{2\tau}{T_2} - \frac{\tau_1}{T_1}\right)} \quad (7)$$

where $A(0)$ is the signal intensity after the first radio frequency (RF) pulse (Figure 12). T_1 and T_2 are the spin-lattice and spin-spin relaxation times, respectively. While measuring the echo signal evolution, τ and τ_1 are fixed, and only the dependence of A as a function of g is analyzed, which is called the diffusion decay.

In the case of non-exponential diffusion decay decays, the experimental curves:

$$A(g) = \frac{A(2\tau, \tau_1, g)}{A(2\tau, \tau_1, 0)}, \quad (8)$$

are usually deconvoluted in several exponential components, which are described by Equation (3). For the multiphase system consisting of m phases in the case of slow (compared to t_d) molecular exchange between the phases:

$$A(g) = \sum_{i=1}^{m} p'_i exp(-\gamma^2 g^2 \delta^2 t_d D_{si}) \quad (9)$$

where D_{si} is the self-diffusion coefficient of the i-th component and:

$$p'_i = p_i \exp\left(-\frac{2\tau}{T_{2i}} - \frac{\tau_1}{T_{1i}}\right) / \sum_{i=1}^{m} p_i exp\left(-\frac{2\tau}{T_{2i}} - \frac{\tau_i}{T_{1i}}\right), \quad \sum_{i=1}^{m} p_i = 1 \quad (10)$$

Here p_i is the relative amount of the nuclei belonging to the molecules characterized by the self-diffusion coefficient D_{si}. The value p_i is called the population of the i-th phase. For the long T_1 and T_2 values, it is usually assumed that $p_i \approx p'_i$. The details of the experimental curve decomposition in several exponential diffusion decays were described previously [44].

We have decomposed diffusion decays on two or three exponential components; the values m in Equation (9) were two or three, accordingly. Between different phases (individual and associated molecules), a molecular exchange occurs. The lifetime in phase is τ. In the case of fast exchange rate $\tau << t_d$ (t_d is diffusion time), the exponential diffusion decay is observed, which is characterized by the average self-diffusion coefficient:

$$D = \Sigma p_i \cdot D_{si} \quad (11)$$

For slow rate exchange conditions, $\tau >> t_d$ multi-exponential diffusion decay shape according to Equation (9) is observed, and p_i and D_{si} do not depend on diffusion time t_d.

If phase exchange time is comparable with diffusion time $\tau \approx t_d$, the slowly moving molecule phase population exponentially decreases with increasing diffusion time, and lifetime τ may be estimated [49,50].

4. Conclusions

The self-organization of a series of differently functionalized fullerene derivatives dissolved in the solvents of different polarity and suspension of RBCs was investigated with pulsed field gradient NMR spectroscopy of ^{1}H, ^{19}F, ^{31}P nuclei. No aggregation was observed for the fullerene derivatives containing nonpolar functional groups **I–V** in carbon disulfide, deuterated chloroform, and toluene-d_8 solutions. The hydrodynamic diameters calculated from Stokes–Einstein equation are equal to individual molecule van der Waals diameters (1.2–1.4 nm). Therefore, Stokes–Einstein model is correct for hydrodynamic size calculations. The fullerene derivatives bearing polar functional groups such as -COOH, -COOK, -P(O)(OH)$_2$, -SO$_3$Na showed a strong tendency to aggregate. The revealed diameters of the aggregates varied from 2.2 nm to 9.6 nm depending on the solvent and temperature. The water-soluble fullerene derivatives **VII–XIII** demonstrated the most stable aggregates with a diameter of about 5 nm. An analysis of the concentration dependences showed that in solutions, the number of associated molecules of water-soluble derivatives of fullerenes increases with increasing concentration. Aggregated lifetimes were estimated from the analysis of diffusion decay shape dependence on the diffusion time. Associate lifetime increases with increasing fullerene derivatives aqueous solution concentration.

Self-diffusion of water-soluble fullerene derivatives **XI–XIII** in RBCs was characterized using ^{1}H PFG NMR. Were obtained and analyzed the diffusion decays of the molecules of compounds **XI–XIII** in a suspension of RBCs. It was found that a fraction of fullerene derivative molecules shows a self-diffusion coefficient of about (5–6)·10^{-12} m^2/s, indepen-

dent of fullerene derivative type, which matched the coefficient of the lateral diffusion of lipids in the RBCs membrane (D_L = (5–7) 10^{-12} m^2/s). This experimental finding evidences the absorption of the fullerene derivatives by RBC. The obtained results suggest that fullerene derivative molecules are probably fixed on the RBC surface. The average lifetime of the fullerene derivative molecule on RBC was estimated as 440 ± 70 ms for compound **XI**, 470 ± 70 ms for compound **XII**, and 1200 ± 300 ms for compound **XIII**. An experimental dependence of the lifetime of molecules of compound **XI** in the RBC membrane on the concentration of the compound in suspension was obtained. It was shown that with increasing concentration, the lifetime also increases.

Thus, pulsed field gradient NMR was shown to be a versatile technique for the investigation of self-organization and interactions of the fullerene derivatives with blood cells, providing essential information which could be projected on their behavior in-vivo after intravenous administration while screening as potential drug candidates.

Author Contributions: Statement of work, writing—review and editing V.I.V.; investigated derivatives of fullerenes A.V.M., O.A.K., E.A.K. and P.A.T.; investigated red blood cells Y.V.S.; experimental work and processing of results A.V.C. and I.A.A. All authors have read and agreed to the published version of the manuscript.

Funding: This research was performed with the support of State Assignment of the Federal Research Center of Problem of Chemical Physics and Medicinal Chemistry RAS (state registration No. 0089-2019-0010/AAAA-A19-119071190044-3 and No. AAAA-A19-119071890015-6).

Acknowledgments: NMR measurements were performed using equipment from the Multi-User Analytical Center of the Federal Research Center of Problem of Chemical Physics and Medicinal Chemistry RAS and Science Center in Chernogolovka, RAS. We are grateful to I.I. Voronov and A.V. Zhilenkov for the synthesis of several fullerene derivatives.

Conflicts of Interest: The authors declare no conflict of interest.

References

1. Langa, F.; Nierengarten, J.-F. *Fullerene Principles and Applications*; RCS: Cambridge, UK, 2007; 398p. [CrossRef]
2. Penkova, A.V.; Acquah, S.F.A.; Piotrovskiy, L.B.; Markelov, D.A.; Semisalova, A.S.; Kroto, H.W. Fullerene derivatives as nano-additives in polymer composites. *Russ. Chem. Rev.* **2017**, *86*, 530. [CrossRef]
3. Nakajima, N.; Nishi, C.; Li, F.-M.; Ikada, Y. Photo-Induced Cytotoxicity of Water-Soluble Fullerene. *Fuller. Sci. Technol.* **1996**, *4*, 1–19. [CrossRef]
4. Tabata, Y.; Ishii, T.; Aoyama, T.; Oki, R.; Hirano, Y.; Ogawa, O.; Ikada, Y. Sonodynamic Effect of Polyethylene glecol-conjugated Fullerene on Tumor. In *Perspectives of Fullerene Nanotechnology*; Osawa, E., Ed.; Kluver Academic Publishers: Amsterdam, The Netherlands, 2001; pp. 185–199.
5. Mashino, T.; Nishikawa, D.; Takanashi, K.; Usui, U.; Yamori, T.; Seki, M.; Endo, T.; Mochizuki, M. Antibacterial and antiproliferative activity of cationic fullerene derivatives. *Bioorg. Med. Chem. Lett.* **2003**, *13*, 4395–4397. [CrossRef] [PubMed]
6. Fernandes, N.B.; Shenoy, R.U.K.; Kajampady, M.K.; DCruz, C.E.M.; Shirodkar, R.K.; Kumar, L.; Verma, R. Fullerenes for the treatment of cancer: An emerging tool. *Environ. Sci. Pollut. Res. Int.* **2022**, *29*, 58607–58627. [CrossRef]
7. Friedman, S.H.; Ganapathi, P.S.; Rubin, Y.; Kenyon, G.L. Optimizing the binding of fullerene inhibitors of the HIV-1 protease through predicted increases in hydrophobic desolvation. *J. Med. Chem.* **1998**, *41*, 2424–2429. [CrossRef]
8. Bosi, S.; Da Ros, T.; Spalluto, G.; Balzarini, J.; Prato, M. Synthesis and anti-HIV properties of new water-soluble bis-functionalized[60]fullerene derivatives. *Bioorg. Med. Chem. Lett.* **2003**, *13*, 4437. [CrossRef]
9. Mashino, T.; Shimotohno, K.; Ikegami, N.; Nishikawa, D.; Okuda, K.; Takanashi, K.; Nakamura, S.; Mochizuki, M. Human immunodeficiency virus-reverse transcriptase inhibition and hepatitis C virus RNA-dependent RNA polymerase inhibition activities of fullerene derivatives. *Bioorg. Med. Chem. Lett.* **2005**, *15*, 1107. [CrossRef]
10. Castro, E.; Garcia, A.H.; Zavalaa, G.; Echegoyen, L. Fullerenes in biology and medicine. *J. Mater. Chem. B* **2017**, *5*, 6523. [CrossRef]
11. Khalikov, S.K.; Sharipova, D.; Zafarov, S.Z.; Umarkhon, M.; Alieva, S.V. Synthesis and Characterization of Fullero-C60 a-Amino Acids with Antiviral Properties. *Chem. Nat. Compd.* **2017**, *53*, 121–127. [CrossRef]
12. Bosi, S.; Da Ros, T.; Castellano, S.; Bafni, E.; Prato, M. Antimycobacterial activity of ionic fullerene derivatives. *Bioorg. Med. Chem. Lett.* **2000**, *10*, 1043–1045. [CrossRef]
13. Su, Y.; Ding, M.; Dong, H.; Hu, Y.; Yang, D.; Shao, J.; Huang, B. Recent advances in nanozymes for combating bacterial infection. *Mater. Chem. Front.* **2022**, *6*, 2596–2609. [CrossRef]

14. Belik, A.Y.; Rybkin, A.Y.; Voronov, I.V.; Goryachev, N.S.; Volyniuk, D.; Grasulevicius, J.V.; Troshin, P.A.; Kotelnikov, A.I. Non-covalent complexes of polycationic fullerene C60 derivative with xanthene dyes—Spectral and photochemical properties in water and in liposomes. *Dyes Pigments* **2017**, *139*, 65–72. [CrossRef]
15. Mikhailov, P.A.; Kraevaya, O.A.; Belik, A.Y.; Rybkin, A.Y.; Khakina, E.A.; Goryachev, N.S.; Usol'tseva, L.I.; Romanenko, Y.V.; Koifman, O.I.; Gushchina, O.I.; et al. Synthesis, photophysical properties, and photochemical activity of the water-soluble dyad based on fullerene C60 and chlorin e6 derivatives. *Dokl. Phys. Chem.* **2017**, *477*, 226–230. [CrossRef]
16. Belik, A.Y.; Rybkin, A.Y.; Goryachev, N.S.; Sadkov, A.P.; Filatova, N.V.; Buyanovskaya, A.G.; Talanova, V.N.; Klemenkova, Z.S.; Romanova, V.S.; Koifman, M.O.; et al. Nanoparticles of water-soluble dyads based on amino acid fullerene C60 derivatives and pyropheophorbide: Synthesis, photophysical properties, and photodynamic activity. *Spectrochim. Acta Part A Mol. Biomol. Spectrosc.* **2021**, *260*, 119885. [CrossRef]
17. Yurkova, A.A.; Khakina, E.A.; Troyanov, S.I.; Chernyak, A.V.; Shmygleva, L.; Peregudov, A.A.; Martynenko, V.M.; Dobrovolskiy, Y.A.; Troshin, P.A. Arbuzov chemistry with chlorofullerene $C_{60}Cl_6$: A powerful method for selective synthesis of highly functionalized [60]fullerene derivatives. *Chem. Commun.* **2012**, *48*, 8916. [CrossRef]
18. Khakina, E.A.; Kraevaya, O.A.; Popova, M.L.; Peregudov, A.S.; Troyanov, S.I.; Chernyak, A.V.; Martynenko, V.M.; Kulikov, A.V.; Scholse, D.; Troshin, P.A. Synthesis of different types of alkoxy fullerene derivatives from chlorofullerene C60Cl6. *Org. Biomol. Chem.* **2017**, *15*, 773–777. [CrossRef]
19. Kraevaya, O.A.; Peregudov, A.S.; Godovikov, I.A.; Shchurik, E.V.; Martynenko, V.M.; Shestakov, A.F.; Balzarini, J.; Schols, D.; Troshin, P.A. Direct arylation of C60Cl6 and C70Cl8 with carboxylic acids: A synthetic avenue to water-soluble fullerene derivatives with promising antiviral activity. *Chem. Commun.* **2020**, *56*, 1179–1182. [CrossRef]
20. Ros, T.D.; Prato, M. Medicinal chemistry with fullerenes and fullerene derivatives. *Chem. Commun.* **1999**, *I.8*, 663–669. [CrossRef]
21. Rokitskaya, T.I.; Antonenko, Y.N. Fullerenol C60(OH)24 increases ion permeability of lipid membranes in a pH-dependent manner. *Biochim. Biophys. Acta* **2016**, *1858*, 1165–1174. [CrossRef]
22. Wattraint, O.; Sarazin, C. Diffusion measurements of water, ubiquinone and lipid bilayer inside a cylindrical nanoporous support: A stimulated echo pulsed-field gradient MAS-NMR investigation. *Biochim. Biophys. Acta* **2005**, *1713*, 65–72. [CrossRef]
23. Leal, C.; Sandström, D.; Nevsten, P.; Topgaard, D. Local and translational dynamics in DNA–lipid assemblies monitored by solid-state and diffusion NMR. *Biochim. Biophys. Acta* **2008**, *1778*, 214–228. [CrossRef] [PubMed]
24. Tardy-Laporte, C.; Arnold, A.A.; Genard, B.; Gastineau, R.; Morançais, M.; Mouget, J.-L.; Tremblay, R.; Marcotte, I. A 2H solid-state NMR study of the effect of antimicrobial agents on intact *Escherichia coli* without mutating. *Biochim. Biophys. Acta* **2013**, *1828*, 614–622. [CrossRef] [PubMed]
25. Grebowski, J.; Krokosz, A.; Puchala, M. Fullerenol C60(OH)36 could associate to band 3 protein of human erythrocyte membranes. *Biochim. Biophys. Acta* **2013**, *1828*, 2007–2014. [CrossRef] [PubMed]
26. Grebowski, J.; Krokosz, A.; Puchala, M. Membrane fluidity and activity of membrane ATPases in human erythrocytes under the influence of polyhydroxylated fullerene. *Biochim. Biophys. Acta* **2013**, *1828*, 241–248. [CrossRef] [PubMed]
27. Chen, M.; Zhou, S.; Guo, L.; Wang, L.; Yao, F.; Hu, Y.; Li, H.; Hao, J. Aggregation Behavior and Antioxidant Properties of Amphiphilic Fullerene C60 Derivatives Cofunctionalized with Cationic and Nonionic Hydrophilic Groups. *Langmuir* **2019**, *35*, 6939–6949. [CrossRef]
28. Harano, K.; Nakamura, E. Interfacial Chemistry of Conical Fullerene Amphiphiles in Water. *Acc. Chem. Res.* **2019**, *52*, 2090–2100. [CrossRef]
29. Li, J.; Chen, M.; Zhou, S.; Li, H.; Hao, J. Self-assembly of fullerene C60-based amphiphiles in solutions. *Chem. Soc. Rev.* **2022**, *51*, 3226–3242. [CrossRef]
30. Nakamura, E.; Isobe, H. Functionalized Fullerenes in Water. The First 10 Years of Their Chemistry, Biology, and Nanoscience. *Acc. Chem. Res.* **2003**, *36*, 807. [CrossRef]
31. Zhang, G.; Liu, Y.; Liang, D.; Gan, L.; Li, Y. Facile Synthesis of Isomerically Pure Fullerenols and Formation of Spherical Aggregates from C60(OH)8. *Angew. Chem. Int. Ed.* **2010**, *49*, 5293. [CrossRef]
32. E, Y.; Bai, L.; Fan, L.; Han, M.; Zhang, X.; Yang, S. Electrochemically generated fluorescent fullerene[60] nanoparticles as a new and viable bioimaging platform. *J. Mater. Chem.* **2011**, *21*, 819–823. [CrossRef]
33. Wang, G.; Zhao, G.; Yan, L. Investigation on the aggregation properties of cationic [60]fullerene derivative. *Chin. Sci. Bull.* **2004**, *49*, 1441. [CrossRef]
34. Liao, Q.; Qu, X.; Chen, L.; Jin, X. Aggregates of Polymer-Substituted Fullerenes. *J. Phys. Chem. B* **2006**, *110*, 7153. [CrossRef] [PubMed]
35. Kato, H.; Böttcher, C.; Hirsch, A. Sugar Balls: Synthesis and Supramolecular Assembly of [60]Fullerene Glycoconjugates. *Eur. J. Org. Chem.* **2007**, *2007*, 2659–2666. [CrossRef]
36. Braun, M.; Hartnagel, U.; Ravanelli, E.; Schade, B.; Böttcher, C.; Vostrowsky, O.; Hirsch, A. Amphiphilic [5:1]- and [3:3]-Hexakisadducts of C60. *Eur. J. Org. Chem.* **2004**, *2004*, 1983–2001. [CrossRef]
37. Avilova, I.A.; Chernyak, A.V.; Zhilenkov, A.V.; Troshin, P.A.; Volkov, V.I. The self-organization of water soluble fullerene derivatives studied by pulsed field gradient NMR. *Mendeleev Commun.* **2016**, *26*, 146. [CrossRef]
38. Hong, Y.S.; Kim, K.C.; Volkov, V.I.; Skirda, V.D.; Lee, C.-H. Structural and dynamic properties of polyoxyethylene sorbitan monooleate micelle in water dispersion studied by pulsed field gradient NMR. *Appl. Magn. Reson.* **2005**, *29*, 351. [CrossRef]

39. Zhu, Y.-Y.; Li, C.; Li, G.-Y.; Jiang, X.-K.; Li, Z.-T. Hydrogen-Bonded Aryl Amide Macrocycles: Synthesis, Single-Crystal Structures, and Stacking Interactions with Fullerenes and Coronene. *J. Org. Chem.* **2008**, *73*, 1745–1751. [CrossRef]
40. Ksenofontov, A.A.; Bichan, N.G.; Khodov, I.A.; Antina, E.V.; Berezin, M.B.; Vyugin, A.I. Novel non-covalent supramolecular systems based on zinc(II) bis(dipyrromethenate)s with fullerenes. *J. Mol. Liq.* **2018**, *269*, 327–334. [CrossRef]
41. Ksenofontov, A.A.; Lukanov, M.M.; Bichan, N.G.; Khodov, I.A.; Kudryakova, N.O.; Ksenofontova, K.V.; Antina, E.V. Non-covalent supramolecular systems with photoinduced electron transfer based on zinc bis(dipyrromethenate)s and C60. *Dyes Pigments* **2021**, *185*, 108918. [CrossRef]
42. Hirao, T.; Fujii, N.; Iwabe, Y.; Haino, T. Self-sorting behavior in supramolecular fullerene polymerization directed by host–guest complexation between calix[5]arene and C60. *Chem. Commun.* **2021**, *57*, 11831–11834. [CrossRef]
43. Chen, S.; Chen, D.; Lu, M.; Zhang, X.; Li, H.; Zhang, X.; Yang, X.; Li, X.; Tu, Y.; Li, C.Y. Incorporating Pendent Fullerenes with High Refractive Index Backbones: A Conjunction Effect Method for High Refractive Index Polymers. *Macromolecules* **2015**, *48*, 8480–8488. [CrossRef]
44. Volkov, V.I.; Chernyak, A.V.; Avilova, I.A.; Slesarenko, N.A.; Melnikova, D.L.; Skirda, V.D. Molecular and Ionic Diffusion in Ion Exchange Membranes and Biological Systems (Cells and Proteins) Studied by NMR. *Membranes* **2021**, *11*, 385. [CrossRef]
45. Gianolio, E.; Ferrauto, G.; Di Gregorio, E.; Aime, S. Re-evaluation of the water exchange lifetime value across red blood cell membrane. *Biochim. Biophys. Acta* **2016**, *1858*, 627–631. [CrossRef] [PubMed]
46. Lindblom, G.; Orädd, G. Lipid lateral diffusion and membrane heterogeneity. *Biochim. Biophys. Acta* **2009**, *1788*, 234–244. [CrossRef] [PubMed]
47. Waldeck, A.R.; Kuchel, P.W.; Lennon, A.J.; Chapman, B.E. NMR diffusion measurements to characterise membrane transport and solute binding. *Prog. Nucl. Magn. Reson. Spectrosc.* **1997**, *30*, 39–68. [CrossRef]
48. Anselmi, C.; Bernardi, F.; Centini, M.; Gaggelli, E.; Gaggelli, N.; Valensin, D.; Valensin, G. Interaction of ferulic acid derivatives with human erythrocytes monitored by pulsed field gradient NMR diffusion and NMR relaxations studies. *Chem. Phys. Lipids* **2005**, *134*, 109–117. [CrossRef]
49. Cho, C.-H.; Hong, Y.-S.; Kang, K.; Volkov, V.I.; Skirda, V.D.; Lee, C.-Y.J.; Lee, C.-H. Water self-diffusion in *Chlorella* sp. studied by pulse field gradient NMR. *Magn. Reson. Imaging* **2003**, *21*, 1009–1017. [CrossRef]
50. Suh, K.-J.; Hong, Y.-S.; Skirda, V.D.; Volkov, V.I.; Lee, C.-Y.; Lee, C.-H. Water self-diffusion behavior in yeast cells studied by pulsed field gradient NMR. *Biophys. Chem.* **2003**, *104*, 121–130. [CrossRef]
51. Avilova, I.A.; Vasil'ev, S.G.; Rimareva, L.V.; Serba, E.M.; Volkova, L.D.; Volkov, V.I. Water metabolism in cells of Saccharomyces cerevisiae of races Y-3137 and Y-3327, according to pulsed-field gradient NMR data. *Russ. J. Phys. Chem. A* **2015**, *89*, 710. [CrossRef]
52. Avilova, I.A.; Smolina, A.V.; Kotelnikov, A.I.; Kotelnikova, R.A.; Loskutov, V.V.; Volkov, V.I. Self-diffusion of water and blood lipids in mouse erythrocytes. *Appl. Magn. Reson.* **2016**, *47*, 335–347. [CrossRef]
53. Avilova, I.A.; Khakina, E.A.; Kraevaya, O.A.; Kotelnikov, A.I.; Kotelnikova, R.A.; Troshin, P.A.; Volkov, V.I. Self-diffusion of water-soluble fullerene derivatives in mouse erythrocytes. *Biochim. Biophys. Acta BBA-Biomembr.* **2018**, *1860*, 1537–1543. [CrossRef] [PubMed]
54. Spernol, A.; Wirtz, K. Zur Mikroreibung in Flüssigkeiten. *Z. Nat. A* **1953**, *8*, 522–532. [CrossRef]
55. Gierer, A.; Wirtz, K. Molekulare Theorie der Mikroreibung. *Z. Nat. A* **1953**, *8*, 532–538. [CrossRef]
56. Perrin, F. Mouvement brownien d'un ellipsoide—I. Dispersion diélectrique pour des molécules ellipsoidales. *J. Phys. Radium* **1936**, *7*, 497–511. [CrossRef]
57. Edward, J.T. Molecular volumes and the Stokes-Einstein equation. *J. Chem. Educ.* **1970**, *47*, 261. [CrossRef]
58. Kawasaki, S.; Aketa, T.; Touhara, H.; Okino, F.; Boltalina, O.V.; Gol'dt, I.V.; Troyanov, S.I.; Taylor, R. Crystal Structures of the Fluorinated Fullerenes C60F36 and C60F48. *J. Phys. Chem. B* **1999**, *103*, 1223. [CrossRef]
59. Chernyak, A.V.; Avilova, I.A.; Khakina, E.A.; Mumyatov, A.V.; Zabrodin, V.A.; Troshin, P.A.; Volkov, V.I. Supramolecular Self-Organization of Fullerene Derivatives in Solutions Studied by Pulsed Field Gradient NMR Technique. *Appl. Magn. Reson.* **2016**, *47*, 859–868. [CrossRef]
60. Mumyatov, A.V.; Susarova, D.K.; Mukhacheva, O.A.; Troshin, P.A.; Razumov, V.F. Fullerene Derivatives with Reduced Electron Affinity and a Photovoltaic Cell Using the Same. European Patent Application No. EP 12180839.8A, 17 August 2012.
61. Mumyatov, A.V.; Goryachev, A.E.; Prudnov, F.A.; Mukhacheva, O.A.; Sagdullina, D.K.; Chernyak, A.V.; Troyanov, S.I.; Troshin, P.A. Monocyclopropanated fullerene derivatives with decreased electron affinity as promising electron acceptor materials for organic solar cells. *Synth. Met.* **2020**, *270*, 116565. [CrossRef]
62. Hummelen, J.C.; Knight, B.W.; LePeq, F.; Wudl, F.; Yao, J.; Wilkins, C.L. Preparation and Characterization of Fulleroid and Methanofullerene Derivatives. *J. Org. Chem.* **1995**, *60*, 532–538. [CrossRef]
63. Voronov, I.I.; Martynenko, V.M.; Chernyak, A.V.; Balzarini, J.; Schols, D.; Troshin, P.A. Synthesis and Antiviral Activity of Water-Soluble Polycarboxylic Derivatives of [60]Fullerene Loaded with 3,4-Dichlorophenyl Units. *Chem. Biodivers.* **2018**, *15*, e1800293. [CrossRef]
64. Hsieh, F.-Y.; Zhilenkov, A.V.; Voronov, I.I.; Khakina, E.A.; Mischenko, D.V.; Troshin, P.A.; Hsu, S.-h. Water-soluble fullerene derivatives as brain drugs: Surface chemistry determines neuroprotective and antitumor effects. *ACS Appl. Mater. Interfaces* **2017**, *9*, 11482–11492. [CrossRef] [PubMed]

65. Khakina, E.A.; Yurkova, A.A.; Peregudov, A.S.; Troyanov, S.I.; Trush, V.; Vovk, A.I.; Mumyatov, A.V.; Martynenko, V.M.; Balzarini, J.; Troshin, P.A. Highly selective reactions of C60Cl6 with thiols for synthesis of functionalized [60]fullerene derivatives. *Chem. Commun.* **2012**, *48*, 7158–7160. [CrossRef] [PubMed]
66. Wong, C.-W.; Zhilenkov, A.V.; Kraevaya, O.A.; Mischenko, D.V.; Troshin, P.A.; Hsu, S.-h. Toward Understanding the Antitumor Effects of Water-Soluble Fullerene Derivatives on Lung Cancer Cells: Apoptosis or Autophagy Pathways? *J. Med. Chem.* **2019**, *62*, 7111–7125. [CrossRef] [PubMed]
67. Anisimov, A. Gradient NMR Method for Studies of Water Translational Diffusion in Plants. *Membranes* **2021**, *11*, 487. [CrossRef] [PubMed]